Mechanistic Studies of an Antibody-Catalyzed Elimination Reaction

Floyd E. Romesberg, Mark E. Flanagan,† Tetsuo Uno,‡ and Peter G. Schultz*

Contribution from the Howard Hughes Medical Institute and Department of Chemistry, University of California, Berkeley, California 94720, Central Research Division, Pfizer Inc., Groton, Connecticut 06340, and Symyx Technologies, 3100 Central Expressway, Santa Clara, California 95051

Received November 13, 1997

Abstract: Catalytic antibody 43D4-3D12, which was generated against the substituted tertiary amine **1**, catalyzes the elimination of HF from β-fluoroketone **2**. We have cloned and produced the antibody as a chimeric Fab and constructed a model of the active site−substrate complex. Mutagenesis studies of the active site indicate that Glu^H50 acts as the general base and suggest that $Tyr96^L$ may also play a role in the elimination reaction. Antibody 43D4-3D12 also efficiently catalyzes the elimination of HBr from substrate **4** by an E2 mechanism, again involving selective abstraction of the proton β-to the nitrophenyl ring by Glu^H50. The antibody-catalyzed reaction affords predominantly the internal olefins, whereas the major product resulting from the uncatalyzed reaction is the alcohol, which arises from the competing substitution reaction. In addition, antibody 43D4-3D12 catalyzes an acetal hydrolysis reaction in which Glu^H50 likely acts as a general acid. These studies point to the success of this particular hapten design strategy in generating an active site with a desired catalytic functional group. They also illustrate the utility of using related reactions as mechanistic probes of biological catalysis.

Introduction

Many enzymatic transformations, including isomerization, elimination, and condensation reactions, involve proton transfeer to and from carbon.[1] Catalytic antibodies have been shown to catalyze many of these same reactions.[2−6] For example, antibody 43D4-3D12, which was generated against positively charged hapten **1**, was found to catalyze the elimination of HF from β-fluoroketone **2** (Figure 1) with a rate enhancement of approximately 10^5 relative to the reaction catalyzed by free acetate in solution.[2] In this case, rather than mimicking the transition state of the reaction, hapten **1** contains an ammonium group designed to elicit a carboxylate residue appropriately positioned to affect catalysis. Chemical modification studies of antibody 43D4-3D12 confirmed that either an aspartate or glutamate residue plays a key role in catalysis, and the pH dependence of the reaction indicated an essential residue with a pK_a of 6.3, active in the deprotonated form. Kinetic isotope effect data are consistent with an E2 or E1cb mechanism.[3] The antibody has also been shown to catalyze regioselective oxime formation between 4-nitroacetophenone and hydroxylamine (Figure 1).[7] This additional catalytic activity is consistent with the presence of an active site carboxylate group that can function as either a general acid or general base.

To further investigate the mechanism and structure of antibody 43D4-3D12, we have cloned, sequenced, and produced the recombinant antibody in *E. coli*. A number of active site mutants were generated based on a model of the antibody−substrate complex, and their catalytic properties were characterized. In addition, we have used a number of alternative chemical reactions as mechanistic probes of the active site (Figure 1). These studies provide additional insights into the requirements and scope of proton transfer in antibody- and enzyme-catalyzed reactions.

Materials and Methods

General Methods. Unless otherwise noted, materials were obtained from commercial suppliers and were used without further purification. Dichloromethane was dried by distillation from CaH_2, and tetrahydrofuran was dried by distillation from Na^0 and benzophenone. All aqueous solutions were prepared from distilled, deionized water. All oxygen or moisture-sensitive reactions were carried out in oven-dried glassware under a positive pressure of nitrogen. Analytical and preparative thin-layer chromatography (PTLC) were performed on precoated silica gel plates (Merck). Flash chromatography was performed using Keiselgel 60 (230−400 mesh) silica gel.

^{1}H NMR spectra of compounds were recorded on a Bruker AM-400 (400 MHz) Fourier-transform NMR spectrometer at the University of California, Berkeley NMR facility. ^{1}H Resonances are reported in units of parts per million downfield from tetramethylsilane (TMS). ^{13}C NMR spectra were recorded on the same instrument; all spectra are proton-decoupled. IR spectra were recorded on a Paragon 500 spectrophotometer (Perkin-Elmer) using NaCl plates. Mass spectra (FAB^+ and EI^+) were recorded at the Mass Spectroscopy Laboratory of the University of California, Berkeley on a VG Zab2EQ or a Kratos MS50 (xenon beam, 7 V) mass spectrometer. Elemental analyses were performed by the Microanalytical Laboratory operated by the College of Chemistry at the University of California, Berkeley. Melting points were determined using a Mel-Temp melting point apparatus and are uncorrected.

4-(4-Nitrophenyl)-2-butanone. To a stirred solution of 1-iodo-4-nitrobenzene (1.0 g, 4.02 mmol) and 3-butene-2-ol (0.363 g, 5.05 mmol) in 10 mL of acetonitrile were added 9 mg (0.040 mmol) of palladium acetate and 0.127 g (1.25 mmol) of triethylamine, and the mixture was heated to reflux for 24 h. The reaction was diluted with ether and

† Pfizer Inc.
‡ Symyx Technologies.

(1) Walsh, C. *Enzymatic Reaction Mechanisms*; W. H. Freeman: New York, 1979.
(2) Shokat, K. M.; Leumann, C.; Sugasawara, R.; Schultz, P. G. *Nature* **1989**, *383*, 269.
(3) Shokat, K.; Uno, T.; Schultz, P. G. *J. Am. Chem. Soc.* **1994**, *116*, 2261.
(4) Reymond, J. L. *Angew. Chem., Int. Ed. Engl.* **1995**, *34*, 2285.
(5) Wagner, J. L.; Lerner, R. A.; Barbas, C. F., III. *Science* **1995**, *270*, 1797.
(6) Jackson, D. Y.; Schultz, P. G. *J. Am. Chem. Soc.* **1991**, *113*, 2319.
(7) Uno, T.; Gong, B.; Schultz, P. G. *J. Am. Chem. Soc.* **1994**, *116*, 1145.

S0002-7863(97)03899-7 CCC: $15.00 © 1998 American Chemical Society
Published on Web 05/15/1998

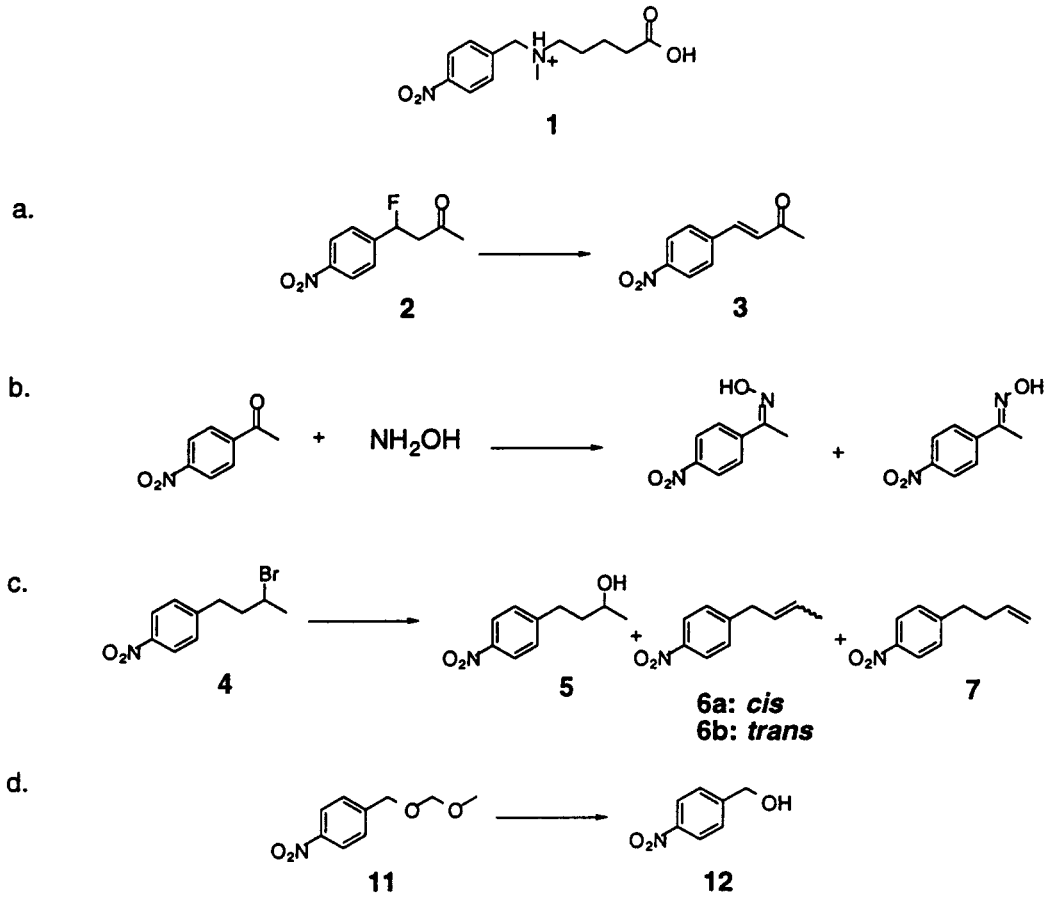

Figure 1. Reactions catalyzed by the antibody 43D4-3D12 which was generated against hapten **1**: (a) β-fluoride elimination;[2] (b) oxime formation;[7] (c) bromide elimination; and (d) acetal hydrolysis.

washed with saturated NH_4Cl (aq), saturated $NaHCO_3$ (aq), water, and saturated brine, then dried over $MgSO_4$ and concentrated to dryness in vacuo. The residue was then purified by flash chromatography (silica; 2:1 hexanes/ethyl acetate) affording 0.7 g of product (92% yield): R_f = 0.41, amber crystals from ethyl acetate/hexanes, mp 37−40 °C; ^{1}H NMR (400 MHz) ($CDCl_3$) δ TMS 2.15 (s, 3H), 2.81 (t, 2H, J = 7.4 Hz), 2.99 (t, 2H, J = 7.3 Hz), 7.34 (d, 2H, J = 8.7 Hz), 8.13 (d, 2H, J = 8.7 Hz); ^{13}C NMR (100 MHz) ($CDCl_3$) δ 29.29, 30.01, 44.13, 123.70, 129.22, 146.49, 148.92, 206.61; IR (NaCl) 2936, 1712, 1598, 1514, 1342, 1169, 856 cm^{-1}; HRMS (FAB), calcd for $C_{10}H_{12}NO_3$ (MH^+) 194.0817, found 194.0780.

4-(4-Nitrophenyl)-2-butanol (5). To a stirred solution of 4-(4-nitrophenyl)-2-butanone (39 mg, 0.202 mmol) in 5 mL of methanol cooled to 0 °C was added 31 mg (0.807 mmol) of $NaBH_4$, and the resulting reaction was stirred at 0 °C for 30 min. The mixture was quenched with 1 N HCl (aq) and concentrated under reduced pressure. The residue was redissolved in dichloromethane, washed with saturated $NaHCO_3$, dried over Na_2SO_4, and concentrated to dryness in vacuo. The crude product was purified by PTLC (silica; 2:1 hexanes/ethyl acetate) affording 35 mg of product as a clear oil (89% yield): R_f = 0.24; ^{1}H NMR (400 MHz) ($CDCl_3$) δ TMS 1.24 (d, 3H, J = 6.2 Hz), 1.72−1.82 (m, 2H), 2.74−2.92 (m, 2H), 3.78−3.86 (m, 1H), 7.35 (d, 2H, J = 8.8 Hz), 8.11−8.14 (m, 2H); ^{13}C NMR (100 MHz) ($CDCl_3$) δ 23.77, 31.98, 40.10, 67.08, 123.62, 129.18, 146.27, 150.15; IR (NaCl): 3369, 2968, 1600, 1517, 1347, 1110, 856 cm^{-1}; HRMS (FAB) calcd for $C_{18}H_{14}NO_3$ (MH^+) 196.0974, found 196.0974.

2-Bromo-4-(4-nitrophenyl)butane (4). To a stirred solution of alcohol **5** (35 mg, 0.179 mmol) in 3 mL of acetonitrile was added 0.118 g (0.357 mmol) of carbon tetrabromide followed by 94 mg (0.357 mmol) of triphenylphosphine, and the resulting mixture was stirred at room temperature for 3 h. Silica gel (4 g) was added and the slurry dried to a powder under reduced pressure. The crude product was then eluted from the silica gel with 2:1 hexanes/ethyl acetate and the eluent concentrated to dryness in vacuo. The residue was purified by PTLC (silica; 4:1 hexanes/ethyl acetate) affording 25 mg of product as a clear oil (54% yield): R_f = 0.53; ^{1}H NMR (400 MHz) ($CDCl_3$) δ TMS 1.74 (t, 3H, J = 6.7 Hz), 2.03-2.16 (m, 2H), 2.83−2.90 (m, 1H), 2.96−3.03 (m, 1H), 4.01−4.07 (m, 1H), 7.35−7.39 (m, 2H), 8.14−8.17 (m, 2H); ^{13}C NMR (100 MHz) ($CDCl_3$) δ 26.47, 33.89, 41.92, 50.02, 123.77, 129.32, 146.56, 148.74; IR (NaCl): 2924, 2863, 1600, 1518, 1346, 1110, 857 cm^{-1}; mass spectrum (EI) m/z 259 (M^+), 257 (M^+). Anal. Calcd for $C_{10}H_{12}BrNO_2$: C, 46.55; H, 4.69; N, 5.43. Found: C, 46.20; H, 4.64; N, 5.29.

***cis*-4-Phenyl-2-butene.** To a stirred solution of benzyl bromide (1.0 g, 5.85 mmol) in 30 mL of THF was added 68 mg (0.059 mmol) of tetrakis(triphenylphosphine)palladium followed by 11.7 mL of a 0.5 M solution of *cis*-propenylmagnesium bromide in THF, and the resulting mixture was stirred at room temperature for 48 h. To the reaction was then added saturated NH_4Cl (aq), and the mixture was extracted with ether. The ether layer was then washed with saturated $NaHCO_3$, water, and saturated brine, dried over $MgSO_4$, and concentrated to dryness in vacuo. The residue was purified by flash chromatography (silica; 50:1 hexanes/ethyl acetate), affording 69 mg of purified product as a liquid (9% purified yield): R_f = 0.33; ^{1}H NMR (400 MHz) ($CDCl_3$) δ TMS 1.73−1.74 (m, 3H), 3.42 (d, 2H, J = 5.1 Hz), 5.59−5.62 (m, 2H), 7.18−7.21 (m, 3H), 7.29 (t, 2H, J = 8.1 Hz).

***cis*-4-(4-Nitrophenyl)-2-butene (6a).** To a stirred solution of *cis*-4-phenyl-2-butene in 1 mL of trifluoroacetic anhydride at 0 °C was added 35 mg (0.151 mmol) of copper(II) nitrate, and the mixture stirred at 0 °C for 30 min, then warmed to room temperature with continued stirring for 2 h. The reaction mixture was poured onto ice, and after the ice melted, the reaction mixture was neutralized with 1 N NaOH followed by extraction with ether. The ether layer was washed with saturated $NaHCO_3$, water, and saturated brine, dried over $MgSO_4$, and concentrated to dryness in vacuo. An aliquot was isolated by semipreparative HPLC (C-18; 55% acetonitrile in H_2O, 4 mL/min;

retention time, 20 min) and concentrated: ^{1}H NMR (400 MHz) ($CDCl_3$) δ TMS 1.71−2.04 (m, 3H), 3.50 (d, 2H, J = 7.3 Hz), 5.52−5.58 (m, 2H), 7.37 (d, 2H, J = 7.8 Hz), 8.13−8.16 (m, 2H); ^{13}C NMR (100 MHz) ($CDCl_3$) δ 12.89, 32.99, 123.67, 126.59, 126.97, 129.08, 131.41, 132.87.

***trans*-4-Phenyl-2-butene.** To a stirred mixture of *trans*-1-bromo-1-propene (500 mg, 4.13 mmol) in 10 mL of THF was added 239 mg (0.207 mmol) of tetrakis(triphenylphosphine)palladium followed by 4.1 mL of a 1 M solution of benzylmagnesium chloride in ether, and the resulting mixture was stirred at room temperature for 24 h. Saturated aqueous NH_4Cl was added followed by ether, and the layers were separated. The organic layer was washed with saturated $NaHCO_3$, water, and saturated brine, dried over $MgSO_4$, and concentrated to dryness in vacuo. The residue was purified by flash chromatography (silica; 50:1 hexanes/ethyl acetate), affording 314 mg of product as a clear liquid (58% yield): R_f = 0.74; ^{1}H NMR (400 MHz) ($CDCl_3$) δ TMS 1.63−1.69 (m, 3H), 3.29 (d, 2H, J = 6.5 Hz), 5.46−5.62 (m, 2H), 7.12−7.17 (m, 3H), 7.22−7.28 (m, 2H); ^{13}C NMR (100 MHz) ($CDCl_3$) δ 17.85, 39.04, 125.84, 126.28, 128.31, 128.45, 130.04, 141.01; IR (NaCl) 3027, 2916, 1494, 1452, 990, 744, 698 cm^{-1}.

***trans*-4-(4-Nitrophenyl)-2-butene (6b).** To a stirred solution of *trans*-4-phenyl-2-butene (162 mg, 1.23 mmol) in 4 mL of trifluoroacetic anhydride at 0 °C was added 142 mg (0.623 mmol) of copper(II) nitrate. The mixture was stirred at 0 °C for 30 min, then warmed to room temperature with continued stirring for 2 h. The reaction mixture was poured onto ice, and after the ice melted, the reaction mixture was neutralized with 1 N NaOH followed by extraction with ether. The ether layer was washed with saturated $NaHCO_3$, water, and saturated brine, dried over $MgSO_4$, and concentrated to dryness in vacuo. An aliquot was then purified by PTLC (silica; 50:1 hexanes/ethyl acetate) (only the tail of band at R_f = 0.32 excised), affording 15 mg of pure **6b** as a liquid: ^{1}H NMR (400 MHz) ($CDCl_3$) δ TMS 1.70−1.72 (m, 3H), 3.41 (br s, 2H), 5.55−5.58 (m, 2H), 7.33 (d, 2H, J = 8.9 Hz), 8.14 (d, 2H, J = 8.7; IR (NaCl) 2915, 1517, 1346 cm^{-1}; HRMS (EI), calcd for $C_{10}H_{11}NO_2$ (M^+) 177.0790, found 177.0786.

4-(4-Nitrophenyl)-1-butene (7). To a stirred solution of trifluoroacetic anhydride (5 mL) at 0 °C containing 0.5 g (3.78 mmol) of 4-phenyl-1-butene (Aldrich) was added 0.44 g (1.89 mmol) of copper(II) nitrate. The resulting mixture was stirred at 0 °C for 30 min, and after warming to room temperature, the reaction mixture was stirred for an additional 2 h, at which point it was poured onto ice. The pH was adjusted to pH 8 with 1 N NaOH (aq) and the mixture extracted 2 × 25 mL with ether. The ether extracts were combined, washed with saturated $NaHCO_3$, water, and saturated brine, then dried over $MgSO_4$ and concentrated to dryness in vacuo. The crude product was purified by flash chromatography (silica; 20:1 hexanes/ethyl acetate), affording 0.54 g of product as an amber liquid (81% yield): R_f = 0.81. An aliquot was then further purified by PTLC (silica; 50:1 hexanes/ethyl acetate): R_f = 0.21 (only top of band excised); ^{1}H NMR (400 MHz) ($CDCl_3$) δ TMS 2.37−2.44 (m, 2H), 2.82 (t, 2H, J = 8.0 Hz), 4.98−5.06 (m, 2H), 5.78−5.86 (m, 1H), 7.32−7.36 (m, 2H), 8.13−8.16 (m, 2H); ^{13}C NMR (100 MHz) ($CDCl_3$) δ 34.72, 35.06, 115.76, 123.47, 129.19, 131.94, 136.77, 146.26; IR (NaCl): 3079, 2936, 2858, 1642, 1606, 1519, 1347, 1110, 996, 916, 859, 744, 698 cm^{-1}; HRMS (FAB), calcd for $C_{10}H_{12}NO_2$ (MH^+) 178.0868, found 178.0826.

4-(4-Nitrophenyl)-2-butanone-*1,1,1,3,3-d*$_5$. To a stirred solution of 4-(4-nitrophenyl)-2-butanone (40 mg, 0.207 mmol) dissolved in 3 mL of methyl alcohol-*d* (Aldrich) was added 10 μL of 40% NaOD in D_2O and the resulting mixture stirred at room temperature for 8 h. The reaction mixture was then concentrated under reduced pressure and the residue purified by PTLC (silica; 2:1 hexanes/ethyl acetate), affording 25 mg of product as an amber oil (61% yield): R_f = 0.40; ^{1}H NMR (400 MHz) ($CDCl_3$) δ TMS: 3.03 (s, 2H), 7.38 (d, 2H, J = 8.6 Hz), 8.16 (d, 2H, J = 8.7 Hz).

2-Bromo-4-(4-nitrophenyl)butane-*1,1,1,3,3-d*$_5$ (8). A stirred solution of 4-(4-nitrophenyl)-2-butanone (25 mg, 0.126 mmol) in 3 mL of methanol-*d* was cooled to 0 °C, and 19 mg (0.504 mmol) of $NaBH_4$ was added. The resulting reaction was stirred at 0 °C for 30 min, then was concentrated under reduced pressure. The residue was triturated with dichloromethane, and the dichloromethane slurry was washed with saturated $NaHCO_3$, dried over Na_2SO_4, and concentrated to dryness in vacuo. The intermediate alcohol was isolated by PTLC (silica; 2:1 hexanes/ethyl acetate), affording 21 mg of liquid product (83% yield): R_f = 0.25. The alcohol was then carried on by reaction in acetonitrile (2 mL) with 83 mg (0.249 mmol) of carbon tetrabromide and 65 mg (0.249 mmol) of triphenylphosphine for 3 h at room temperature. Silica gel (4 g) was added and the slurry dried to a powder under reduced pressure. The crude product was then eluted from silica gel with 2:1 hexanes/ethyl acetate and the eluent concentrated to dryness in vacuo. The residue was purified by PTLC (silica; 4:1 hexanes/ethyl acetate), affording 16 mg of product as a clear oil (49% yield): R_f = 0.53; ^{1}H NMR (400 MHz) ($CDCl_3$) δ TMS 2.85 (1/2 ABq, 1H, J = 13.7 Hz), 2.98 (1/2 ABq, 1H, J = 13.9 Hz), 4.02 (s, 1H), 7.33−7.38 (m, 2H), 8.12−8.22 (m, 2H); ^{13}C NMR (400 MHz) ($CDCl_3$) δ 22.57, 33.71, 43.86, 50.01, 123.78, 129.32, 146.55, 148.75; IR (NaCl): 2950, 1600, 1518, 1346, 1199, 1110, 848 cm^{-1}; mass spectrum (EI) *m*/*z* 264 (M^+), 262 (M^+). Anal. Calcd for $C_{10}H_7D_5BrNO_2$: C, 45.64; H, 4.60; N, 5.32. Found: C, 45.98; H, 4.63; N, 5.48.

4-(4-Acetamidophenyl)-2-butanone. To a stirred solution of 4-acetamidoiodobenzene (1.0 g, 3.83 mmol) and 3-butene-2-ol (0.346 g, 4.81 mmol) in 10 mL of acetonitrile was added 9 mg (0.038 mmol) of palladium acetate and 0.121 g (1.19 mmol) of triethylamine, and the mixture was heated to reflux for 24 h. The reaction was diluted with ether and washed with saturated NH_4Cl (aq), saturated $NaHCO_3$ (aq), water, and saturated brine, then dried over $MgSO_4$ and concentrated to dryness in vacuo. The residue was purified by flash chromatography (silica; 4:1 ethyl acetate/hexanes) affording 0.42 g of product: R_f = 0.35. White crystals were precipitated from ethyl acetate/hexanes, mp 109−111 °C: ^{1}H NMR (400 MHz) ($CDCl_3$) δ TMS 2.13 (s, 3H), 2.15 (s, 3H), 2.73 (t, 2H, J = 7.4 Hz), 2.85 (t, 2H, J = 7.4 Hz), 7.12 (d, 2H, J = 8.3 Hz), 7.40 (d, 2H, J = 8.4 Hz), 7.61 (br s, 1H); ^{13}C NMR (100 MHz) ($CDCl_3$) δ 24.41, 29.07, 30.07, 45.07, 120.17, 128.71, 136.02, 136.88, 168.40, 208.04; IR (NaCl) 3295, 1707, 1665, 1604, 1550, 1515, 1411, 1370, 1321, 824 cm^{-1}. Anal. Calcd for $C_{12}H_{15}NO_2$: C, 70.22; H, 7.37; N, 6.82. Found: C, 69.82; H, 7.40; N, 6.70.

4-(4-Acetamidophenyl)-2-butanol. To a stirred solution of (4-acetamidophenyl)-2-butanone (150 mg, 0.731 mmol) in 15 mL of methanol cooled to 0 °C was added 110 mg (2.92 mmol) of $NaBH_4$. The resulting reaction was stirred at 0 °C for 30 min, then quenched with 1 N HCl (aq) and concentrated under reduced pressure. The residue was redissolved in dichloromethane, washed with saturated $NaHCO_3$, dried over Na_2SO_4, and concentrated to dryness in vacuo. The crude product was purified by recrystallization from ethyl acetate/hexanes, affording 127 mg of product as a white crystalline solid (84% yield), mp 132−135 °C; ^{1}H NMR (400 MHz) (DMSO-d_6) δ HOD 1.02 (d, 3H, J = 6.2 Hz), 1.49−1.58 (m, 2H), 1.98 (s, 3H), 2.42−2.59 (m, 2H), 3.50−3.56 (m, 1H), 4.40 (d, 1H, J = 4.8 Hz), 7.05 (d, 2H, 8.4 Hz), 7.41 (d, 2H, J = 8.4 Hz), 9.79 (s, 1H); ^{13}C NMR (100 MHz) (DMSO-d_6) δ 23.26, 23.55, 30.62, 40.57, 64.83, 118.68, 127.96, 136.59, 136.63, 167.62; IR (NaCl) 3292, 2926, 1665, 1604, 1545, 1514, 1412, 1371, 1321, 824 cm^{-1}. Anal. Calcd for $C_{12}H_{17}NO_2$: C, 69.53; H, 8.26; N, 6.76. Found: C, 69.42; H, 8.34; N, 6.70.

4-(4-Acetamidophenyl)-2-bromobutane (10). To a stirred solution of 4-(4-acetamidophenyl)-2-butanol (30 mg, 0.145 mmol) in 2 mL of acetonitrile was added 96 mg (0.289 mmol) of carbon tetrabromide followed by 76 mg (0.289 mmol) of triphenylphosphine. The resulting mixture was stirred at room temperature for 3.5 h, silica gel (4 g) was then added, and the slurry was dried to a powder under reduced pressure. The crude product was then eluted from the silica gel with 2:1 ethyl acetate/hexanes and the eluent concentrated to dryness in vacuo. The residue was purified by PTLC (silica; 3:1 ethyl acetate/hexanes), affording 12 mg of product (32% yield): R_f = 0.57; ^{1}H NMR (400 MHz) ($CDCl_3$) δ TMS 1.72 (d, 3H, J = 6.6 Hz), 1.96−2.14 (m, 2H), 2.16 (s, 3H), 2.67−2.86 (m, 2H), 4.02−4.08 (m, 1H), 7.14 (d, 2H, J = 8.4 Hz), 7.35 (br s, 1H), 7.41 (d, 2H, J = 8.4 Hz); ^{13}C NMR (100 MHz) ($CDCl_3$) δ 24.53, 26.49, 33.33, 42.61, 50.75, 120.16, 129.01, 135.93, 136.95, 169.14; IR (NaCl): 3284, 3120, 2922, 1661, 1601, 1514, 1409, 1320, 838, 763 cm^{-1}.

***O*-Methanesulfonyl-4-(4-nitrophenyl)-2-butanol (9).** To a stirred solution of alcohol **5** (40 mg, 0.205 mmol) in 10 mL of dichloromethane

cooled to 0 °C was added 70 mg (0.615 mmol) of methanesulfonyl chloride followed by 104 mg (1.02 mmol) of triethylamine, and the resulting mixture was stirred at 0 °C for 30 min, then at room temperature for 2 h. The reaction was washed with water, dried over Na_2SO_4, and concentrated to dryness in vacuo, affording 54 mg of product (96% yield): ^{1}H NMR (400 MHz) ($CDCl_3$) δ TMS 1.47 (d, 3H, J = 6.3 Hz), 1.65−2.11 (m, 2H), 2.79−2.91 (m, 2H), 3.04 (s, 3H), 4.84−4.89 (m, 1H), 7.37 (d, 2H, J = 8.8 Hz), 8.14−8.18 (m, 2H).

4-((Methoxymethoxy)methyl)nitrobenzene (11). To a stirred solution of dichloromethane (10 mL) containing 100 mg (0.653 mmol) of 4-nitrobenzyl alcohol was added 79 mg (0.980 mmol) of chloromethyl methyl ether followed by 253 mg (1.96 mmol) of *N*,*N*-diisopropylethylamine, and the resulting mixture was stirred at room temperature for 18 h. The reaction was diluted with dichloromethane, washed with saturated $NaHCO_3$, dried over Na_2SO_4, and concentrated to dryness in vacuo. The residue was then purified by preparative TLC (silica; 1:1 ethyl acetate/hexanes), affording 37 mg of product as a yellow oil (29% yield): R_f = 0.4; ^{1}H NMR (100 MHz) ($CDCl_3$) δ TMS 3.41 (s, 3H), 4.69 (s, 2H), 4.74 (s, 2H), 7.52 (d, 2H, J = 8.9 Hz), 8.20 (d, 2H, J = 8.7 Hz); ^{13}C NMR (400 MHz) ($CDCl_3$) δ 55.55, 67.94, 96.12, 123.60, 127.81, 145.61, 147.35. IR (NaCl): 2942, 2889, 1723, 1607, 1522, 1348, 1151, 1107, 1050, 847, 739 cm^{-1}; HRMS (FAB) calcd for $C_9H_{12}NO_4$ (MH^+) 198.0766, found 198.0741.

***O*-Tetrahydropyranyl-4-nitrobenzyl Alcohol (13).** To a stirred solution of 4-nitrobenzyl alcohol (500 mg, 3.26 mmol) in 30 mL of dichloromethane was added 411 mg (4.89 mmol) of 3,4-dihydro-2*H*-pyran followed by 31 mg (0.163 mmol) *p*-toluenesulfonic acid monohydrate. The resulting mixture was stirred at room temperature for 2 h, then diluted with dichloromethane, washed with saturated $NaHCO_3$, dried over Na_2SO_4, and concentrated to dryness in vacuo affording 743 mg of product as a yellow liquid (96% yield): ^{1}H NMR (400 MHz) ($CDCl_3$) δ TMS 1.55−1.93 (m, 6H), 3.54−3.59 (m, 1H), 3.86−3.92 (m, 1H), 4.61 (1/2 ABq, 1H, J = 13.5 Hz), 4.74 (t, 1H, J = 3.5 Hz), 4.89 (1/2 ABq, 1H, J = 13.5 Hz), 7.52−7.55 (m, 2H), 8.19−8.22 (m, 2H); ^{13}C NMR (400 MHz) ($CDCl_3$) δ 19.18, 25.26, 30.36, 62.18, 67.52, 98.21, 123.46, 123.46, 127.66, 127.66, 146.07, 147.16; IR (NaCl) 2944, 2870, 1607, 1520, 1345, 1126, 1036, 973, 739 cm^{-1}; HRMS (EI) calcd $C_{12}H_{16}NO_4$ (MH^+) 238.1079, found 238.1072.

Antibody (Fab, 43D4-3D12) Expression, Purification, and Mutagenesis. Total RNA was isolated from the hybridoma cell line by the method of Chomczynski and Sacchi.[8] Total RNA was enriched for messenger RNA encoding 43D4-3D12 variable regions by affinity chromatography with oligo(dT) cellulose (Pharmacia). Constant region 3′ primers were used to reverse transcribe cDNA. PCR amplification with the 3′ constant region primer and the 5′ primers described by Huse *et al.*[9] yielded sufficient DNA for cloning and sequencing. After determination of the J_κ and J_H regions used by 43D4-3D12, 3′ primers corresponding to the appropriate J regions and containing restriction sites were synthesized and used in conjunction with the 5′ primers to PCR amplify DNA corresponding to the variable regions of 43D4-3D12. The V_H and V_L genes were cloned into plasmid p4X.[10] This construct fuses the murine V_H and V_L genes to human C_H1 and $C_\kappa1$ constant regions, respectively. Mutagenesis was performed by the method of Kunkel.[11] Sequence determination was performed by the method of Sanger.[12] The Fab fragments were isolated from *E. coli* 25F2 transformed with the appropriate plasmids, according to the published protocol.[10] Fab fragments were further purified by protein G affinity chromatography (Sepharose CL-6B, Pierce). The Fab fragments were concentrated and stored in either kinetics buffer or phosphate-buffered saline (Ca^{2+}, Mg^{2+} free, deionized water).

Kinetics and Product Analysis. UV kinetic measurements of the fluoride elimination reaction were carried out as described previously.[2] High-pressure liquid chromatography (HPLC) kinetic measurements were determined using a Rainin SD-200 binary HPLC system equipped with a Rainin UV-1 UV detector and a Rainin C-18 Microsorb analytical column (4.6 mm × 25 cm). Initial velocities were determined by measuring integrated product peak differences as a function of time (corrected for background) and comparing to authentic standard calibration curves. Bromide elimination reactions were carried out using 10 μM Fab as determined by $OD_{280\ nm}$ (1.37 absorbance units for 1.0 mg/mL of 43D4-3D12 and a molecular weight of 50 000) in 50 mM sodium phosphate monobasic buffer (adjusted to pH 8.0 with 2 N NaOH) containing 10% acetonitrile (37 °C) at substrate concentrations ranging from 50 to 250 μM. Products were analyzed by reverse phase HPLC (C-18, 55% acetonitrile in 50 mM sodium acetate, pH 5.0, 1 mL/min, 254 nm detection) over 30 min. Retention times for the *cis* (**6a**), *trans* (**6b**), and terminal olefin (**7**) products were 21.5, 22.7, and 19.9 min, respectively. The retention time for the alcohol product (**5**) was 4.7 min. Acetal hydrolyses were carried out using 10 μM Fab in 50 mM sodium acetate, 50 mM NaCl (pH 5.0), and 5% acetonitrile (37 °C) at substrate concentrations ranging from 20 μM to 4 mM. Products were analyzed by reverse phase HPLC (C-18, 60% acetonitrile in 50 mM sodium acetate, pH 5.0, 254-nm detection) over 15 min. Kinetic analyses of uncatalyzed reactions were carried out in the absence of antibody, but under otherwise identical conditions.

Homology Model of Fab 43D4-3D12. The generation of a model of the Fab 43D4-3D12 variable region is possible due to the existence of conserved antibody framework regions, an experimental crystallographic database of canonical loop structures whose conformations depend on well-defined residues,[13] and experimental constraints. An initial model of Fab 43D4-3D12 was generated using the AbM program.[14] Briefly, coordinates corresponding to the most homologous framework regions (1baf and 1bbj, respectively), as well as for canonical loops L2, H1, and H2 (L2, class 1; H1, class 1; H2, class 2), were selected from an antibody data base. Side chains were then changed to those corresponding to 43D4-3D12 using maximum overlap. f Coordinates for the noncanonical loops were selected by combined conformational and Cα database searching. The hypervariable loops were preminimized with several hundred iterations using the steepest-descents algorithm within the program Discover.[15] Substrates **2**, **4**, and **11** were docked manually, employing the following experimental constraints. First, it was assumed that the *p*-nitrophenyl group would be oriented into the binding pocket. During immunization, hapten **1** was conjugated to keyhole limpet hemocyanin (KLH) via a linker, and this orientation for hapten binding is the only one allowing the antibody to approach hapten. We assume that the substrate binds analogously. This is supported by several crystal structures of *p*-nitrophenyl complexes.[16,17] Second, the acidic protons were positioned proximate to the catalytic residue. Several exploratory steepest-descents minimizations of the hypervariable loops were started from various initial conformations. The binding pocket of the lowest energy structure was then minimized by a combination of steepest-descent and conjugate-gradient methods to a root mean square derivative less than 0.001 kcal/(mol·Å). Multiple substrate orientations were examined, including those corresponding to *syn* and *anti* deprotonation, as well as those leading to *cis* and *trans* products.

Results and Discussion

Cloning and Production of Fab 43D4-3D12. The sequences of the 43D4-3D12 V_L and V_H chains are shown in Figure 2. V_L possesses the highest homology to the $V_\kappa21$ group as

(8) Chomczynski, P. and Sacchi, N. *Anal. Biochem.***1987**, *162*, 156.
(9) Huse, W. D.; Sastry, L.; Kang, S. A.; Alting-Mees, M.; Burton, D. R.; Benkovic, S. J.; Lerner, R. A. *Science* **1989**, *246*, 1275.
(10) Ulrich, H. D.; Patten, P. A.; Yang, P. L., Romesberg, F. E.; Schultz, P. G. *Proc. Natl. Acad. Sci. U.S.A.* **1995**, *88*, 8784.
(11) Kunkel, T. A.; Roberts, J. D.; Zakour, R. A. *Methods in Enzymol.***1987**, *154*, 367.
(12) Sanger, W.; Nicklen, S.; Coulson, A. R. *Proc. Natl. Acad. Sci. U.S.A.* **1977**, *74*, 5463.
(13) Chothia, C.; Lesk, A. M. *J. Mol. Biol.* **1987**, *196*, 901.
(14) Oxford Molecular, 1994.
(15) Biosym Technologies, 1992.
(16) Patten, P. A.; Gray, N. S.; Yang, P. L.; Marks, C. B., Wedemayer, G. L.; Boniface, J. J.; Stevens, R. C.; Schultz, P. G. *Science* **1996**, *271*, 1086.
(17) Hsieh-Wilson, L. C.; Schultz, P. G.; Stevens, R. C. *Proc. Natl. Acad. Sci. U.S.A.* **1996**, *93*, 5363.

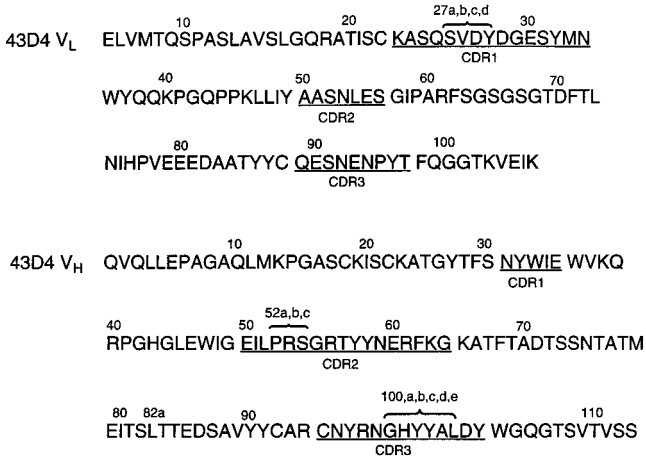

Figure 2. Amino acid sequences of 43D4-3D12 light and heavy chain variable regions (V_L and V_H). Hypervariable regions are underlined.

delineated by Potter *et al.*[18,19] and is joined in frame to $J_\kappa 2$. The nucleotide sequence of the 43D4-3D12 V_H shows that the antibody uses a germline gene from the V_H1 (J558) family[20,21] along with J_H4. While the 43D4-3D12 V_H chain appears to contain a significant number of somatic mutations, it is interesting to note that the catalytic Glu50^H (see below) is present in the majority of the germline genes and therefore probably does not represent a somatic mutation.

The recombinant 43D4-3D12 was produced in *E. coli* as chimeric Fab possessing murine variable regions fused to human constant regions C_H1 and $C_\kappa 1$. The wild-type (wt) protein expression levels were found to be low, relative to a variety of other catalytic antibodies expressed similarly[10] (approximately 100 μg/L). The catalytic constants of the recombinant Fab 43D4-3D12, $k_{cat} = 0.30$ min^{-1} and $K_M = 214$ μM at pH 6.5, are indistinguishable from those of the fully murine antibody.[2]

In the course of mutagenesis studies of 43D4-3D12 (see below), several active site mutants were generated by site directed mutagenesis, e.g., each residue of the CDR3 loop (residues 92−96) was mutagenized to alanine, histidine, and lysine. Surprisingly, 11 mutants corresponding to either alanine, histidine, or lysine at positions 92−94 and either histidine or lysine (not alanine or phenylalanine) at position 96 resulted in a greater than 1 order of magnitude increase in protein expression levels relative to wt protein. Given that two of three wt codons were present in the DNA encoding each mutant, low expression of the recombinant wt protein is not likely a consequence of codon usage. Additionally, control experiments were performed by generating silent mutations in the same residues of the wt antibody. In all cases low protein expression levels were found. It is possible that the increased expression levels of the mutant proteins result from the removal of deleterious interactions involving the light chain CDR3 loop in either the folded protein (light chain CDR3 residues supply approximately 20% of the light chain contacts with the heavy chain) or in some intermediate folded state.[22]

Mutagenesis and Modeling Studies. Previous affinity labeling experiments indicated that the likely active site general base is either Glu46 or Glu50 of the heavy chain.[3] To unequivocally assign the catalytic residue, both glutamate residues were mutated to glutamine by site-directed mutagenesis. The mutants were then assayed for their ability to catalyze fluoride elimination from substrate **2**. The Glu46^{H}Gln mutant retained full catalytic activity, $k_{cat} = 0.30$ min^{-1} and $K_m = 214$ μM at pH 6.5, while the Glu50^{H}Gln mutant had no measurable activity above the background reaction. We therefore assign Glu50^H as the catalytic carboxylate residue which acts as an efficient general base catalyst. Glu50^H was also mutated to a histidine to probe the stereoelectronic requirements for proton transfer. The Glu50^{H}His mutant also possessed no catalytic activity above background at pH 6.5, possibly arising from poor alignment of the basic imidazole nitrogen with the Cα protons.

In an attempt to gain insight into the structural basis for the catalytic properties of 43D4-3D12 a computational model of the Fab was generated. The model is based on the high structural homology between antibody framework regions and a crystallographic database of antibodies sharing canonical loop structures with Fab 43D4-3D12.[13] Additionally, experimental constraints allow for the positioning of the substrate in the antibody combining site. Specifically, the active site base Glu50^H is positioned so that it is in close proximity to the acidic CH group of substrate **2** and the nitroaryl ring is oriented into the binding pocket in a manner consistent with the geometry of the hapten-KLH conjugate used to elicit antibody 43D4-3D12.

The modeled Michaelis complex between substrate **2** and Fab 43D4-3D12 is shown in Figure 3. The model predicts that the substrate interacts with residues in the active site of 43D4-3D12 via both hydrogen bonding and hydrophobic packing interactions. Residues from L3, H1, H2, and H3 all participate in forming a deep, occluded binding pocket for the substrate. At the bottom of the pocket the *p*-nitro group of **2** is hydrogen bonded to the indole ring of Trp47^H and the carboxamide group of Asn89^L. The side chains of Tyr96^L and Cys95^H pack against the phenyl moiety of the substrate. Both enantiomers position the fluoride leaving group to form a hydrogen bond to the hydroxyl group of Tyr96^L, which could facilitate loss of the fluoride by stabilizing developing negative charge in the transition state. Minimization of both complexed enantiomers with substrate geometries corresponding to either a *syn*- or *anti*-fluoride elimination reaction resulted in isoenergetic minima, with all complexes maintaining the hydrogen bond between the fluoride group and Tyr96^L. The only stable conformation of the incipient olefin was found to be *trans*, consistent with the experimental result.[2] Aromatic residues, predominately Trp33^H, Tyr97^H, and Tyr100c^H are predicted to limit access of water to the binding pocket. With the exception of Asn94^L, all of the side chains in close proximity to the catalytic Glu50^H are hydrophobic, consistent with the elevated pK_a of Glu50^H observed experimentally. The hydrophobic, tightly packed substrate environment is also consistent with the unsuccessful attempts to catalyze the exchange of deuterium for hydrogen in *p*-nitrobenzyl acetone when bound to antibody 43D4-3D12.

The above model suggests that residues 92−96 of the light chain CDR3 loop are proximal to Glu50^H. In an effort to modulate the activity of 43D4-3D12, each of these residues was mutagenized to alanine, histidine, and lysine, and the catalytic activity of the mutant Fab was assayed using β-fluoroketone **2** as a substrate. The activity of the antibody was remarkably invariant to substitutions at residues 92−94. All three of the

(18) Potter, M.; Newell, J. B.; Rudikoff, S.; Haber, E. *Mol. Immunol.* **1982**, *19*, 1.
(19) Heinrich, G.; Traunecker, A.; Tonegawa, S., *J. Exp. Med.* **1984**, *159*, 417.
(20) Dildrop, R. *Immunol. Today* **1984**, *5*, 85.
(21) Brodeur, P. H.; Riblet, R. *Eur. J. Immunol.* **1984**, *14*, 922.
(22) (a) Dul, J. L.; Argon, Y. *Proc. Natl. Acad. Sci. U.S.A.* **1990**, *87*, 8135. (b) Dul, J. L.; Burrone, O. R.; Argon, Y. *J. Immunol.* **1992**, *127*, 2609. (c) Wu, G. E.; Hozumi, N.; Murialdo, H. *Cell* **33**, 77. (d) Martin, T. M.; Kowalczyk, C.; Stevens, S.; Wiens, G. D.; Stenzel-Poore, M. P.; Rittenberg, M. B. *J. Immunol.* **1996**, *157*, 4341.

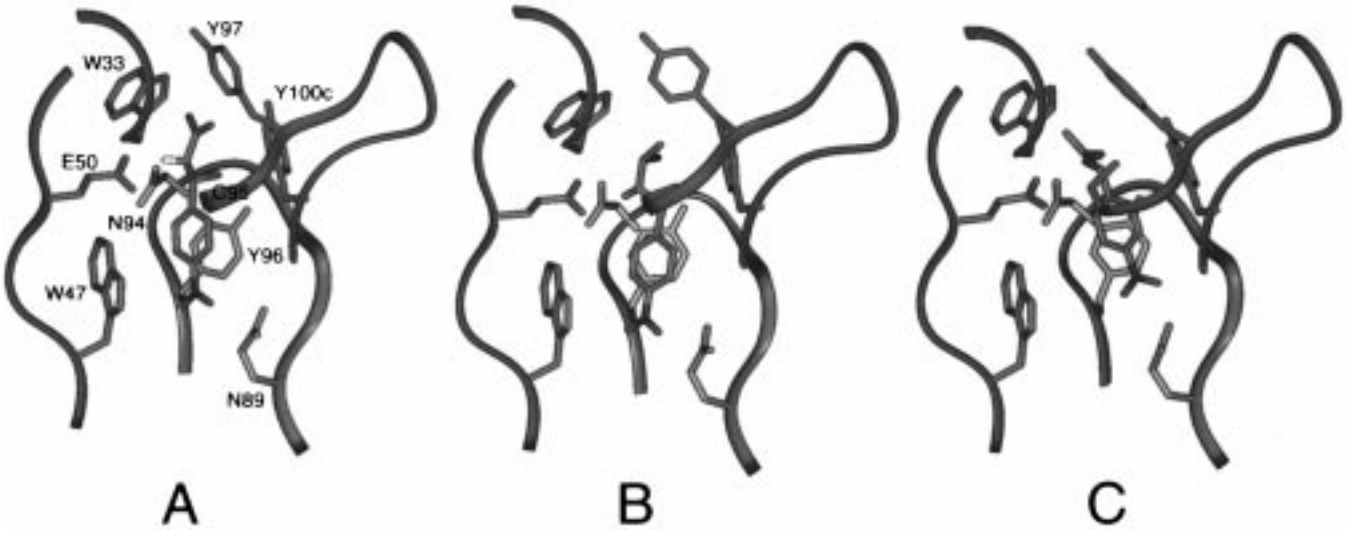

Figure 3. Modeled Michaelis complex of 43D4-3D12 and (A) substrate **2** in *anti-trans* configuration; (B) substrate **4** in *syn-cis* configuration; and (C) substrate **11**. The antibody heavy and light chains are colored purple and orange, respectively. Critical antibody side chains are labeled with their single-letter notation. The substrates are colored according to atom: carbon is green, nitrogen is blue, oxygen is red, fluoride is grey, and bromide is brown.

alanine mutants, the histidine mutants at position 92 and 94, as well as the lysine mutant at position 92, had approximately 75% of wt specific activity at pH 6.5. Histidine and lysine mutations at position 93 resulted in catalysts with approximately 30% of wt antibody specific activity. The mutant with lysine at position 94 was approximately 20% more active than wt antibody between pH 5.8 and 6.5. Thus, it is likely that these residues do not significantly perturb the active site structure or reactivity of $Glu50^H$.

To evaluate the potential contributions of π-stacking and hydrogen bond donation to the substrate leaving group, which are both predicted by the modeled Michaelis complex, we mutagenized $Tyr96^L$ to alanine, histidine, lysine, and phenylalanine. At pH 6.5, the $Tyr96^L$Phe mutant catalyzed the fluoride elimination from substrate **2** at a rate within a factor of 2 of that for wild-type 43D4-3D12: $k_{cat} = 0.17$ min^{-1} and $K_M = 120$ μM. It appears that the predicted hydrogen bond does not contribute significantly to catalysis, or alternatively, the predicted interaction of $Tyr96^L$ with the substrate may be incorrect. However, mutation of $Tyr96^L$ to Ala, His, or Lys led to the complete loss of catalytic activity. Thus, the residue may make important van der Waals packing interactions with the substrate, but does not appear to stabilize the transition state by hydrogen bonding interactions.

Characterization of the Antibody-Catalyzed Bromide Elimination Reaction. It has been shown that an antibody can catalyze a number of different reactions if the substrates share a common recognition element (e.g., nitrophenyl ring) and the reactions have overlapping mechanistic requirements (e.g., a general base).[4,7] Indeed, analysis of the catalytic activity of an antibody using different reactions can provide important mechanistic and structural insights. We therefore assayed the ability of Fab 43D4-3D12 to catalyze the dehydrobromination reaction of substrate **4** (Figure 1), which lacks acidic protons α to the leaving group. Consequently, this elimination reaction is not likely to involve an E1cb mechanism, but rather an E2 or E1 mechanism. There is also a competing solvolysis pathway in the corresponding acetate-catalyzed reaction which yields, in addition to the *cis* and *trans* internal olefins **6a**,**b** and the terminal olefin **7**, the substitution product, alcohol **5**, in a product ratio of 6% (**6a**), 14% (**6b**), 5% (**7**), and 75% (**5**), respectively. In the dehydrobromination reaction, the position of the leaving group (bromide) relative to the nitrophenyl ring is shifted in comparison to that of the fluoride group in **2**. Consequently, if the nitrophenyl group orients the substrate in a similar way in the antibody active site, $Glu50^H$ should be positioned to catalyze the elimination reaction to afford the unconjugated olefin products **6a**,**b**.

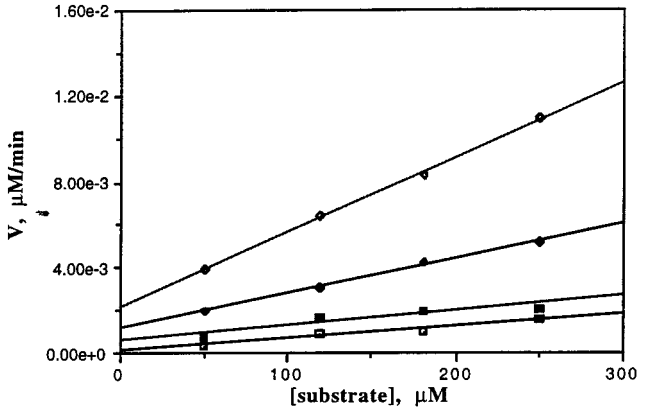

Figure 4. Kinetics and deuterium isotope effects for *cis* and *trans* eliminations of **4** and **8**: (open diamonds) *trans* elimination of protio substrate; (closed squares) *trans* elimination of deutero substrate; (closed diamonds) *cis* elimination of protio substrate; (open squares) *cis* elimination of deutero substrate. All reactions were carried out in 50 mM phosphate buffer and 10% acetonitrile, pH 8.0 (37 °C), for 24 h in the presence of 10 μM Fab (43D4-3D12) and are background corrected.

Initial rates for the antibody-catalyzed reaction were determined at concentrations of substrate **4** ranging from 50 to 250 μM in the presence of 10 μM Fab (50 mM phosphate buffer and 10% acetonitrile, pH 8.0 for 24 h at 37 °C). Analysis of the reactions rates (v) for formation of **6a** and **6b** over background as a function of substrate concentration afforded the apparent second-order rate constants (k_{cat}/K_M) of 1.6 and 3.5 M^{-1} min^{-1} for the *cis* and *trans* elimination reactions, respectively (Figure 4). The limited solubility of **4** under the reaction conditions precluded independent determination of k_{cat} and K_m.

These reaction rates can be compared to the corresponding second-order rate constants for the acetate-catalyzed reactions under the same conditions of 7.1×10^{-6} and 7.4×10^{-6} M^{-1}

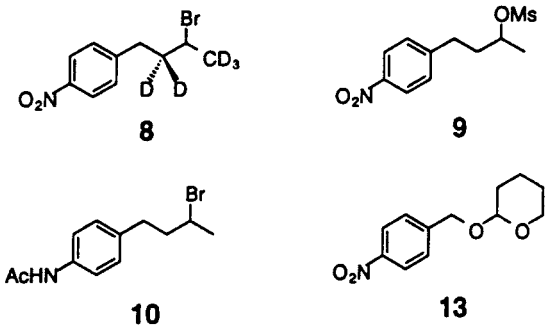

Figure 5. Mechanistic probes of 43D4-3D12 (see text).

min^{-1} for the *cis* and *trans* elimination reactions, respectively. This results in a ratio of second-order rate constants $((k_{cat}/K_m)/k_{-OAc})$ of 2.2×10^5 for the *cis* elimination reaction and 4.8×10^5 for the *trans* elimination reaction, showing the antibody to be an efficient catalyst for these reactions. Furthermore, antibody 43D4-3D12 selectively catalyzes the formation of internal olefins **6a** (18%) and **6b** (72%) relative to terminal olefin **7** (1%) and alcohol **5** (9%) (corrected for the uncatalyzed reaction). In contrast, the alcohol resulting from the competing substitution reaction is the major product of the uncatalyzed reaction. Thus, the antibody-catalyzed reaction is again selective for abstraction of the proton β- to the aryl ring, whose position corresponds to that of the ammonium group in hapten **1**. Moreover the competing solvolysis reaction is not significantly catalyzed by the antibody, indicating that the antibody selectively stabilizes the transition state for the elimination reaction relative to the substitution reaction, even under aqueous conditions. This suggests that water is restricted from the 43D4-3D12 active site, consistent with the model described above in which the side chains of residues $Trp33^H$, $Tyr97^H$, and $Tyr100c^H$ sequester the substrate from solvent.

Isotope effect experiments were carried out with the pentadeutero substrate **8**. The ratios of the second-order rate constants $(k_{cat}/K_m)_H/(k_{cat}/K_m)_D$ were found to be 2.9 and 4.1 for the *cis* and *trans* elimination reactions, respectively. These kinetic isotope effects indicate a significant contribution of an E2-like transition state to the elimination reaction. In the case of substrate **2**, delineating between an E2 or an E1cb mechanism was not possible due to the acidity of the protons α to the carbonyl group. With substrate **4**, however, the pK_a's of the homobenzylic protons are sufficiently high to make an E1cb mechanism for the bromide elimination unlikely. As was the case in the fluoride elimination reaction, no catalysis was observed for substrate **4** in the case of the $Glu50^HGln$ mutant, demonstrating the importance of the $Glu50^H$ carboxylate group in the E2 elimination of bromide from substrate **4**.

Mesylate **9** and bromide **10** (Figure 5) were also examined as potential substrates for antibody 43D4-3D12. Both uncatalyzed elimination reactions proceeded with measurable rates in aqueous buffer to yield olefin products. However, neither reaction was accelerated over background in the presence of antibody 43D4-3D12, demonstrating high substrate specificity of the antibody toward the hapten programmed recognition elements.

We also modeled substrate **4** into the combining site of antibody 43D4-3D12 (Figure 3). As with the 43D4-3D12 substrate **2** complex, substrate **4** is predicted to bind in a deep hydrophobic pocket with the *p*-nitro group hydrogen bonded to the indole ring of $Trp47^H$ and the carboxamide group of $Asn89^L$. The side chains of $Tyr96^L$ and $Cys95^H$ pack against the phenyl moiety of the substrate, and $Trp33^H$, $Tyr97^H$ and $Tyr100c^H$ sequester the substrate from water. This is consistent with the antibody's demonstrated ability to selectively catalyze bromide elimination relative to solvolysis. The bromide leaving group is not predicted to hydrogen bond to an active site residue. Docking of both substrate enantiomers in geometries corresponding to either the *syn*- or *anti*-bromide elimination reaction followed by minimization led to distinct but nearly isoenergetic minima. Additionally, both *cis* and *trans* conformations of the incipient olefin were found to be roughly equal in energy, consistent with the above described experiments.

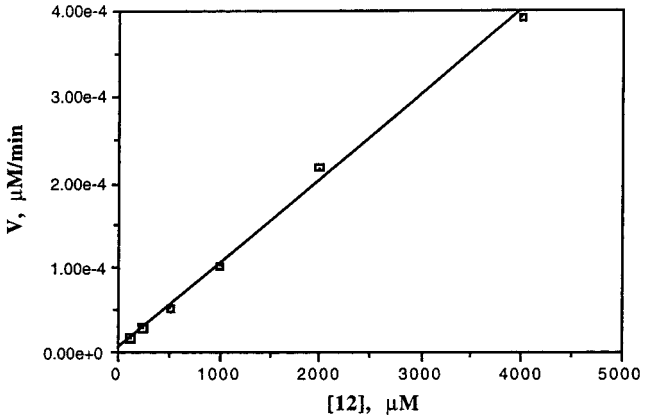

Figure 6. Catalysis of the hydrolysis of acetal **11** by 43D4-3D12. Reactions were carried out in 50 mM NaOAc, 50 mM NaCl, and 5% acetonitrile (pH 5.0) at 37 °C for 24 h in the presence of 10 μM Fab 43D4-3D12.

Antibody-Catalyzed Acetal Hydrolysis Reaction. We also investigated the ability of antibody 43D4-3D12 to catalyze the hydrolysis of acetal **11** (Figure 1). Again, this substrate shares a nitrophenyl recognition element with hapten **1**. However, in this case, it was expected that $Glu50^H$ might act as a general acid to protonate the benzylic oxygen, facilitating expulsion of the benzyl alcohol leaving group. The resulting carboxylate anion could stabilize the positively-charged oxocarbonium ion intermediate. Indeed, it has been shown previously that haptens containing positively-charged ammonium ions can lead to the generation of antibodies capable of catalyzing the hydrolysis of acetal bonds.[23]

At pH 5 acetal **11** has a slow but measurable background rate in 50 mM NaOAc, 50 mM NaCl, and 5% acetonitrile buffer at 37 °C. Initial reaction rates for the antibody-catalyzed reaction were determined under the same conditions at concentrations of **11** ranging from 125 μM to 4 mM in the presence of 10 μM Fab. Analysis of the reactions rates (v) of the antibody-catalyzed formation of alcohol **12** (Figure 1) as a function of substrate concentration afforded an apparent second-order rate constant (k_{cat}/K_M) of 1×10^{-2} M^{-1} min^{-1}. The limited solubility of **11** under the reaction conditions precluded determination of k_{cat} and K_M. This reaction rate can be compared to the second-order rate constant of 1.1×10^{-6} M^{-1} min^{-1} for the reaction catalyzed by acetic acid. The ratio $(k_{cat}/K_M)/k_{HOAc}$ is 8.8×10^3, showing antibody 43D4-3D12 to be an effective catalyst. Antibody 43D4-3D12 was also assayed with THP acetal substrate **13** (Figure 5). The antibody did not catalyze the hydrolysis, again demonstrating substrate specificity.

(23) (a) Yu, J.; Hsieh, L.; Kochersperger, L.; Yonkovich, S.; Stephens, J. C.; Gallop, M. A.; Schultz, P. G. *Angew. Chem., Int. Ed. Engl.* **1994**, *33*, 339. (b) Reymond, J. L.; Janda, K. D.; Lerner, R. A. *Angew. Chem., Int. Ed. Engl.* **1991**, *30*, 1771. (c) Yu, J. and Schultz, P. G. *J. Chem. Soc., Chem. Commun.*, in press. (d) Janda, K. D.; Lo, L.-C.; Shin, M.-M.; Wang, R.; Wong, C.-H.; Lerner, R. A. *Science* **1997**, *275*, 945. (e) Yu, J.; Choi, S. Y.; Moon, K.-D.; Chung, H.-H.; Youn, H. J.; Jeong, S.; Park, H.; Schultz, P. G. *Proc. Natl. Acad. Sci. U.S.A.*, in press.

The modeled Michaelis complex between 43D4-3D12 and substrate **11** is shown in Figure 3. Again the substrate is predicted to bind in a deep hydrophobic pocket with the *p*-nitro group hydrogen bonded to the carboxamide group of $Asn89^{L}$ and the side chains of $Tyr96^{L}$ and $Cys95^{H}$ packing on the substrate phenyl ring. The protonated $Glu50^{H}$ is predicted to hydrogen bond to the benzylic oxygen of substrate **11** consistent with the catalytic mechanism described above. The δ-oxygen is predicted to accept a hydrogen bond from $Asn94^{L}$ which is the only other hydrophilic residue positioned in the 43D4-3D12 combining site.

Conclusion. These studies underscore the ability to introduce a catalytic residue into an antibody combining site that can function as a general acid or a general base by using an appropriately designed immunogen. In the case of antibody 43D4-3D12, the side chain of $Glu50^{H}$ catalyzes both elimination and acetal hydrolysis reactions. The ability of the antibody to catalyze the elimination reaction of substrate **4** over the competing substitution reaction under aqueous reaction conditions again points to the degree to which the antibody active site can control chemical reactivity.

Acknowledgment. This work was supported by the Director, Office of Energy Research, Office of Basic Energy Sciences, Division of Material Sciences, and also by the Division of Energy Biosciences of the U.S. Department of Energy under Contract No. DE-AC03-76SF00098. M.E.F. acknowledges a fellowship from the National Institutes of Health (Grant No. 1F32AI09093-01A1). P.G.S. is a Howard Hughes Medical Institute Investigator and a W. M. Keck Foundation Investigator. We gratefully acknowledge Jodie Chin for assistance with Figure 3.

JA9738992